

# Can Gamma-Ray Bursts Be Used to Measure Cosmology? A Further Analysis

D. Xu<sup>1</sup>, Z. G. Dai<sup>1</sup>, and E. W. Liang<sup>1,2,3</sup>

<sup>1</sup>*Department of Astronomy, Nanjing University, Nanjing 210093, China*

<sup>2</sup>*Department of Physics, Guangxi University, Nanning 530004, China*

<sup>3</sup>*Department of Physics, University of Las Vegas, Nevada 89154, USA*

## ABSTRACT

Two different methods of measuring cosmology with gamma-ray bursts (GRBs) have been proposed since a tight relation between the energy of a GRB jet ( $E_{\gamma, \text{jet}}$ ) and its peak energy of the  $\nu F_{\nu}$  spectrum measured in the cosmological rest frame ( $E'_p$ ), i.e.,  $(E_{\gamma, \text{jet}}/10^{50} \text{ergs}) = C(E'_p/100 \text{keV})^a$ , was recently reported, where  $a$  and  $C$  are dimensionless parameters. In Method I, this relation is recalibrated as cosmology varies. We apply this method to a latest high-redshift sample of 17 observed GRBs, and obtain  $\Omega_M = 0.16^{+0.46}_{-0.14}$  at the  $1\sigma$  confidence level for a flat universe. Furthermore, we make simulations on the basis of the observed GRB sample to study the ability of a cosmological probe by using a sample of 157 pseudo bursts, being comparable to the gold sample of type-Ia supernovae (SNe Ia), and obtain  $\Omega_M = 0.29^{+0.20}_{-0.04}$  ( $1\sigma$ ) for a flat universe, which is consistent with the cosmic concordance model of  $\Omega_M = 0.27$ ,  $\Omega_{\Lambda} = 0.73$  ( $\chi^2_{\text{dof}} = 176.00/155 \approx 1.14$ ). In Method II, this relation is considered to be cosmology-independent, as in the well-known SN cosmology. With this potential “standard candle” relation in nine representative sets of  $(a, C)$ , we find that each set gives different constraints on cosmology for 17 observed bursts. We also consider the relation with  $a \sim 1.5$  and  $C \sim 1.0$  as an example for the cosmological test, because (i) this relation, in principle, can be suggested either from the standard synchrotron mechanism in relativistic shocks combined with the leading afterglow jet model or from the dissipative photosphere models; (ii) the Hubble diagram of GRBs is consistent with that of SNe Ia; and (iii) among the nine cases, such a relation gives the minimum value of the best-fit  $\chi^2$  on the distance modulus. We obtain the mass density  $\Omega_M = 0.18^{+0.18}_{-0.02}$  ( $1\sigma$ ) for a flat universe with a cosmological constant, and  $w = -0.98^{+0.44}_{-0.75}$  ( $1\sigma$ ) with a prior

---

<sup>1</sup>Email: dzg@nju.edu.cn

of  $\Omega_M = 0.27 \pm 0.04$  for an assumed static equation of state of dark energy,  $P = w\rho c^2$ . These results are consistent with the cosmic concordance model of  $\Omega_M = 0.27$ ,  $\Omega_\Lambda = 0.73$  ( $\chi^2_{\text{dof}} = 18.63/15 = 1.24$ ). In addition, our simulated pseudo-GRB sample provides evidence for both the cosmic acceleration at the present time and the transition from past deceleration to present acceleration at a high confidence level. Future observations on GRBs by space-based instruments, including the *HETE-2* and *Swift* satellites, are expected to calibrate  $a$  and  $C$  with a low-redshift sample (i.e.,  $z < 0.1$ ) and thus Method II would be favored; if not, Method I could also provide unique constraints with a large sample. In any case, the *GRB Cosmology* would progress from its infancy into childhood.

*Subject headings:* gamma rays: bursts — cosmology: observations—cosmology: distance scale

## 1. Introduction

The traditional cosmology has been revolutionized by modern sophisticated observation techniques in distant Type Ia supernovae (SNe Ia) (e.g., Riess et al. 1998; Schmidt et al. 1998; Perlmutter et al. 1999; also see Filippenko 2004 for a recent review), cosmic microwave background (CMB) fluctuations (e.g., Bennett et al. 2003; Spergel et al. 2003), and large-scale structure (LSS) (e.g., Daly & Guerra 2002). Modern cosmology has now convincingly suggested that the global mass-energy budget of the universe, and thus its dynamics, is dominated by a dark energy component, and the currently accelerating universe has once been decelerating (e.g. Freedman et al. 2001; Tonry et al. 2003; Kirshner et al. 2003; Riess et al. 2004; Tegmark et al. 2004). The cosmography and the nature of dark energy (including its evolution with redshift, if any) are one of the most important issues in physics and astronomy today. Each type of cosmological data trends to play a unique role in measuring cosmology.

Cosmic gamma-ray bursts (GRBs) are the most intense explosions observed so far. They are believed to be detectable up to a very high redshift (Lamb & Reichart 2000; Ciardi & Loeb 2000; Bromm & Loeb 2002), and their high energy photons are almost immune to dust extinction. These advantages would make GRBs an attractive probe for cosmology. Some attempts on this issue have been made. Schaefer (2003) advocated a new method of measuring cosmology with GRBs (hereafter Method I) by considering two luminosity indicators, which relate the peak luminosity with the spectral lag and the variability for nine GRBs with known redshifts, and gave the constraint on the mass density  $\Omega_M < 0.35$  ( $1\sigma$ ). In this method, both luminosity indicators are recalibrated in every cosmology, and the best

cosmology is obtained by minimizing a  $\chi^2$  statistic. Dai, Liang & Xu (2004) proposed a different method (hereafter Method II) by employing a tight relation between the beaming-corrected  $\gamma$ -ray energy ( $E_{\gamma, \text{jet}}$ ) and the peak energy of the  $\nu F_\nu$  spectrum measured in the cosmological rest frame ( $E'_p$ ), i.e.,  $(E_{\gamma, \text{jet}}/10^{50} \text{ ergs}) = C(E'_p/100 \text{ keV})^a$ , which was recently found by Ghirlanda, Ghisellini & Lazzati (2004a, GGL relation hereafter), and suggested that the mass density of the universe  $\Omega_M = 0.35 \pm 0.15$  ( $1\sigma$ ) for a flat universe with a cosmological constant, and the  $w$  parameter of an assumed static dark-energy equation of state  $w = -0.84 \pm 0.57$  ( $1\sigma$ ), assuming that a relation of  $(a, C) \sim (1.5, 1.1)$  should be intrinsic. These results are consistent with those from other techniques. Method II has been usually adopted in the *SN cosmology*. Following Schaefer's method, Ghirlanda et al. (2004b) and Friedman & Bloom (2004) also used the GGL relation to investigate the same issue but obtained some inconsistent results.

To measure cosmology, a standard candle is required. Finding out a standard candle from the SN Ia sample is a great task. In the beginning of SN Ia cosmology history, the peak brightness of SNe Ia, which was determined by a cosmology-independent approach (e.g. with Cepheid variables, Branch & Miller 1993), was regarded as a perfect “standard candle”. However, this notion had to be given up for the later realization that SNe Ia do not constitute a perfect homogeneous class (e.g. Filippenko 1997a, b). New “standard candle” relations were then put forward to determine the apparent distance moduli (DM) of SNe Ia: the Phillips relation (Phillips 1993); the “multi-color light curve shape” method (Riess, Press, & Kirshner 1996); and the “stretch” method (Perlmutter et al. 1997; Goldhaber et al. 2001), and make SNe Ia a key role in modern cosmology. The procedure of SN Cosmology is summarized as follows: (1) a “standard candle” relation (also called intrinsic relation) is calibrated by using those well-observed nearby SNe Ia, which are independent of cosmic models; (2) this relation is applied to all the other low and high redshift SNe Ia to calculate their apparent DMs on the consideration that such an intrinsic relation is epoch-independent; and (3) the cosmological parameters are constrained by minimizing  $\chi^2$  based on the observations and theoretical models.

Similarly, finding out a “standard candle” relation from the GRB data is becoming more and more attractive and promising. From a standard energy reservoir of GRBs (Frail et al. 2001), the luminosity-variability (or spectral lag) relation (Fenimore & Ramirez-Ruiz 2000; Norris, Marani, & Bonnell 2000), and the isotropic-equivalent energy-peak energy relation (Amati et al. 2002) to the GGL relation (Ghirlanda et al. 2004a), GRBs seem to be towards a more standardizable candle. Similar to the brightness of SNe Ia, the energy reservoirs in GRB jets are narrowly clustered (Frail et al. 2001, see also Bloom et al. 2003), which suggests that GRBs could be a potential “standard candle”. Bloom et al. (2003) plotted several Hubble diagrams with assumed standard energy reservoirs on GRB jets, but found

that the current GRB sample cannot place meaningful constraints on cosmology because of the large dispersion of  $E_{\gamma,\text{jet}}$ , which might be caused by the inhomogeneous origin of the bursts. The two luminosity relations with the variability and spectral lag make GRBs a distance indicator in the same sense as Cepheids and SNe Ia, in which an observed light-curve property can yield the luminosity and then an apparent DM (e.g., Schaefer 2003). Amati et al. (2002) found a relation between the isotropic-equivalent energy radiated in GRBs ( $E_{\gamma,\text{iso}}$ ) and  $E'_p$ , i.e.,  $E_{\gamma,\text{iso}} \propto E'_p^k$  (where  $k \sim 2$ ), by using 12 BeppoSAX bursts. Sakamoto et al. (2004) and Lamb et al. (2004) found the HETE-2 observations not only confirm this relation, but also extend it to X-ray flashes. In addition, it holds among BATSE bursts (Lloyd-Ronning & Ramirez-Ruiz 2002), as well as within a GRB (Liang, Dai & Wu 2004). Physical explanations of this correlation are involved in the standard synchrotron mechanism in relativistic shocks (Zhang & Mészáros 2002; Dai & Lu 2002), the dissipative photosphere models (Rees & Mészáros 2004), and the emission from off-axis relativistic jets (Yamazaki, Ioka & Nakamura 2004; Eichler & Levinson 2004). Because of a large dispersion, this relation cannot give useful information about cosmography.

Fortunately, the GGL relation has such a small dispersion that GRBs become a promising probe of cosmology. In this work, we will carry out a further analysis on the ability of measuring cosmology with GRBs based on current observations and simulations with both methods discussed above. We show that, with Method II, each set of nine representative  $(a, C)$  gives different constraints on the fundamental cosmological quantities for 17 observed bursts. We especially consider the relation with  $a \sim 1.5$  and  $C \sim 1.0$  as an example, both because this case can in principle be suggested either from the standard synchrotron mechanism in relativistic shocks combined with the leading afterglow jet model (Dai et al. 2004) or from the dissipative photosphere models (Rees & Mészáros 2004), and because the Hubble diagram of GRBs is consistent with that of SNe Ia (see section 3 in this paper). In addition, such a relation gives the minimum value of the best-fit  $\chi^2$  on the distance modulus among the nine cases. Since the current observed GRB sample is a bit small, we will also perform a simulation analysis.

This paper is arranged as follows. In section 2, we describe our analytical method. The results based on the current GRB sample are presented in section 3. In sections 4, we perform Monte Carlo simulations on an observational foundation to give predictive constraints on the cosmological parameters with methods I and II, respectively. Conclusions and discussion are presented in section 5.

## 2. Analysis Method

According to the relativistic fireball model, the emission from a spherically expanding shell and from a jet would be rather similar to each other, if the observer is along the jet’s axis and the Lorentz factor of the fireball is larger than the inverse of the jet’s half-opening angle  $\theta$ ; but when the Lorentz factor drops below  $\theta^{-1}$ , the jet’s afterglow light curve is expected to present a break because of sideways expansion (Rhoads 1999; Sari, Piran & Halpern 1999). Therefore, together with the assumptions of the initial fireball emitting a constant fraction  $\eta_\gamma$  of its kinetic energy into the prompt  $\gamma$ -rays and a constant circum-burst density medium of number density  $n$ , the jet’s half-opening angle is given by

$$\theta = 0.161 \left( \frac{t_{j,d}}{1+z} \right)^{3/8} \left( \frac{n_0 \eta_\gamma}{E_{\gamma,iso,52}} \right)^{1/8} \quad (1)$$

where  $E_{\gamma,iso,52} = E_{\gamma,iso}/10^{52}$  ergs,  $t_{j,d} = t_j/1$  day,  $n_0 = n/1$  cm $^{-3}$ . The value of  $\eta_\gamma$  is taken as 0.2 throughout this paper (Frail et al. 2001). The “bolometric” isotropic-equivalent  $\gamma$ -ray energy of a GRB is given by

$$E_{\gamma,iso} = \frac{4\pi d_L^2 S_\gamma k}{1+z}, \quad (2)$$

where  $S_\gamma$  is the fluence (in units of erg cm $^{-2}$ ) received in an observed bandpass and the quantity  $k$  is a multiplicative correction of order unity relating the observed bandpass to a standard rest-frame bandpass (1-10 $^4$  keV in this paper) (Bloom, Frail & Sari 2001). The energy release of a GRB jet thus is given by

$$E_{\gamma,jet} = (1 - \cos \theta) E_{\gamma,iso}. \quad (3)$$

The GGL relation is

$$(E_{\gamma,jet}/10^{50}$$
 ergs) =  $C(E'_p/100$  keV) $^a$  (4)

where  $a$  and  $C$  are dimensionless parameters. Combining equations (1)-(4) and assuming<sup>1</sup>  $\theta \ll 1$ , we approximate the apparent luminosity distance of a GRB as

$$d_L = 7.69 \frac{(1+z)C^{2/3}[E_p^{obs}(1+z)/100]^{2a/3}}{(kS_\gamma t_{j,d})^{1/2}(n_0 \eta_\gamma)^{1/6}} \text{ Mpc} \quad (5)$$

with the uncertainty being

$$\left( \frac{\sigma_{d_L}}{d_L} \right)^2 = \left( \frac{\sigma_k}{2k} \right)^2 + \left( \frac{\sigma_{S_\gamma}}{2S_\gamma} \right)^2 + \left( \frac{\sigma_{t_{j,d}}}{2t_{j,d}} \right)^2 + \left( \frac{\sigma_{n_0}}{6n_0} \right)^2 + \left( \frac{2a}{3} \frac{\sigma_{E_p^{obs}}}{E_p^{obs}} \right)^2$$

---

<sup>1</sup>This assumption is valid because  $|(1 - \cos \theta - \theta^2/2)/(1 - \cos \theta)| < 1\%$  when  $\theta < 0.35$ , and  $< 0.4\%$  when  $\theta < 0.22$ .

$$+ \left( \frac{2}{3} \frac{\sigma_C}{C} \right)^2 + \left( \frac{2a}{3} \frac{\sigma_a}{a} \ln \frac{E_p^{obs}(1+z)}{100} \right)^2 \quad (6)$$

. The apparent DM of a burst can thus be given by

$$\mu_{obs} = 5 \log d_L + 25 \quad (7)$$

with the uncertainty of

$$\sigma_{\mu_{obs}} = \frac{5}{\ln 10} \frac{\sigma_{d_L}}{d_L}. \quad (8)$$

We constrain cosmology with GRB observations by a minimizing  $\chi^2$  technique, which is

$$\chi^2 = \sum_i \left( \frac{\mu_{th,i} - \mu_{obs,i}}{\sigma_{\mu_{obs,i}}^2} \right)^2 \quad (9)$$

where  $\mu_{th}$  is the theoretical DM for a given cosmic model.

### 3. Measuring cosmology with current GRB observations

#### 3.1. Sample Analysis

The great diversity in GRB phenomena suggests that the GRB population may consist of substantially different subclasses (e.g. MacFadyen & Woosley 1999; Bloom et al. 2003; Sazonov et al. 2004; Soderberg et al. 2004). To make GRBs a standard candle, a homogenous GRB sample is required. The most prominent observational evidence for a GRB jet is its temporal break in their afterglow light curves. For some bursts, e.g., GRB030329, their temporal breaks are observed in both the optical and radio bands. Berger et al. (2003) argued that these two breaks are caused by the narrow component and wide component of the jet in this burst, respectively, indicating that the physical origins of the breaks in the optical band and in the radio band are different. In addition, the radio afterglow light curves fluctuate significantly. For example, in the case of GRB970508, the light curve of its radio afterglow does not present clearly a break. Only a lower limit of  $t_j > 25$  days was proposed by Frail et al. (2000). Furthermore, the light curve of its optical afterglow is proportional to  $t^{-1.1}$ , in which case no break appears (Galama et al. 1998). We thus include only those bursts that their temporal breaks in optical afterglow light curves were well measured in our analysis. We obtain a sample of 17 GRBs excluding GRB970508. They are listed in Table 1 with the following headings: GRB name, redshift, the observed peak energy and its error (in

keV), the spectral indices of  $\alpha$  and  $\beta$ , fluence in an observational gamma-ray band and its error (in  $10^{-6}\text{erg/cm}^2$ ), bandpass of observation (in keV), break time (in days), circum-burst medium density and its error (in  $\text{cm}^{-3}$ ), and references.

We correct the observed fluence in a given bandpass to a “bolometric” bandpass of  $1 - 10^4$  keV with spectral fitting parameters. Spectral fittings to observations in different energy bands for one burst may present different results. This difference may significantly affect the bolometric correction. We thus collect the fluence and the spectral fitting parameters from the same original literature as possible. For GRB 970828, GRB 980703, GRB 991216, and GRB 020124, the fluence and the spectral parameters are unavailable from one original literature, so we choose their fluences measured in the widest energy band available in the literature.<sup>2</sup>

For GRB 011211, we approximately take the high-energy spectral index  $\beta$  to be  $-2.3$  for an unavailable spectral index in Amati (2004). The spectra of GRB020124, GRB020813, GRB021004, GRB030226 and XRF030429 are found by the *HETE-II* satellite and not fitted by the Band function but the cutoff power law model. However, it is appropriate that their corresponding “bolometric” fluences are calculated by the latter model with  $\beta \sim -2.3$ , taking into account the potential bias of detecting disability in high-energy bands for the *HETE-II* bursts.

The medium densities of several bursts in our sample have been obtained from broad-band modelling of the afterglow emission (e.g., Panaiteescu & Kumar 2002). For the bursts with unknown  $n$ , we take  $n \simeq 3\text{cm}^{-3}$  with an error of 0.3 (Ghirlanda et al. 2004a and references therein).

### 3.2. Cosmological Constraints

With the data in Table 1, we investigate the GGL relation in various cosmic models. We calculate the  $E_{\gamma,\text{jet}}$  by using equations (1)-(3), and the uncertainty of  $E_{\gamma,\text{jet}}$  is obtained by using the exact error propagation formula. The half-opening angles of all the bursts are less than 0.2 rad in the cosmic concordance model and even less than 0.22 rad in any cosmic

---

<sup>2</sup>It should be noted here that we have also corrected some wrong data in Ghirlanda et al. (2004b) and Friedman & Bloom (2004). For example, (i) the peak energy  $E_p^{\text{obs}}$  of GRB021004 cited by Friedman & Bloom (2004) has been corrected in Sakamoto et al. (2004), (ii) the  $E_p^{\text{obs}}$  of GRB020405 should be 192.5 keV (Price et al. 2003) after correctly understanding the reported energy parameter of the Band function as the break energy  $E_b$  rather than the characteristic energy  $E_0$ .

model.<sup>3</sup> The typical scatters of  $a$  and  $C$  in various cosmic models are 5% and 10%, and the values of  $a$  and  $C$  are in the ranges of [1.40, 1.68] and [0.70, 1.30], respectively. Thus, for the purpose of universality, we select nine representative sets from the combinations of  $a = (1.4, 1.5, 1.6)$  and  $C = (0.8, 1.0, 1.2)$  to test the ability of a cosmological probe from current GRB data.

### 3.2.1. Cosmological Constant

The luminosity distance in a Friedmann-Robertson-Walker (FRW) cosmology with mass density  $\Omega_M$  and vacuum energy density (i.e., the cosmological constant)  $\Omega_\Lambda$  is

$$d_L = c(1+z)H_0^{-1}|\Omega_k|^{-1/2}\text{sinn}\{|\Omega_k|^{1/2} \times \int_0^z dz[(1+z)^2(1+\Omega_M z) - z(2+z)\Omega_\Lambda]^{-1/2}\}, \quad (10)$$

where  $\Omega_k = 1 - \Omega_M - \Omega_\Lambda$ , and “sinn” is  $\sinh$  for  $\Omega_k > 0$  and  $\sin$  for  $\Omega_k < 0$  (Carroll, Press & Turner 1992). For  $\Omega_k = 0$ , equation (10) degenerates to be  $c(1+z)H_0^{-1}$  times the integral. The above equation gives the theoretical DM  $\mu_{\text{th}} = 5 \log(d_L/10 \text{ pc})$ . The likelihood for the cosmological parameters (e.g.  $\Omega_M$  and  $\Omega_\Lambda$ ) can be determined from a  $\chi^2$  statistic as follows

$$\chi^2(h, \Omega_M, \Omega_\Lambda; a, C) = \sum_i \left[ \frac{\mu_{\text{th}}(z_i; h, \Omega_M, \Omega_\Lambda) - \mu_{\text{obs},i}(a, C)}{\sigma_{\mu_{\text{obs},i}}(a, C)} \right]^2 \quad (11)$$

where  $\mu_{\text{obs},i}$  and  $\sigma_{\mu_{\text{obs},i}}$  are calculated by Eqs. 5-8. For the GRBs in our sample, typical error terms of equation (6) are  $\sigma_k/2k \sim 0.025$ ,  $\sigma_{S_\gamma}/2S_\gamma \sim 0.050$ ,  $\sigma_{t_{j,d}}/2t_{j,d} \sim 0.098$ ,  $\sigma_{n_0}/6n_0 \sim 0.038$ ,  $(2a/3)(\sigma_{E_p^{\text{obs}}}/E_p^{\text{obs}}) \sim 0.171$ ,  $(2/3)(\sigma_C/C) \sim 0.067$ , and  $(2a/3)(\sigma_a/a)(\ln[E_p^{\text{obs}}(1+z)/100]) \sim 0.058$ . For  $\sigma_a/a$  and  $\sigma_C/C$ , we take 0.05 and 0.1, being equal to the typical scatters of the GGL relation in various cosmic models. We see that, the dominant error terms are the last three terms. According to the above typical errors, we find the typical uncertainty in the apparent DM for GRBs is  $\sim 0.50$ , which is about twice of that in SNe Ia.

For a given cosmic model  $(\Omega_M, \Omega_\Lambda)_i$ , we calculate the  $\chi^2_i$ , and then calculate the likelihood by  $P \propto e^{-\chi^2/2}$  with marginalization over the Hubble constant  $h$  in the range of  $h \in [0.68, 0.75]$  (Bennett et al. 2003). The contours of the likelihood intervals from  $1\sigma$  to  $3\sigma$  in the  $\Omega_M$ - $\Omega_\Lambda$  plane for the nine cases are shown in Figure 1. The value of  $\chi^2_{\text{min}}$  in each scenario is also marked in the corresponding panel. The best-fit  $(\Omega_M, \Omega_\Lambda)$  pair and the

---

<sup>3</sup> $\Omega_M$  and  $\Omega_\Lambda$  are taken from 0 to 1.

constraints on  $\Omega_M$  for a flat universe with a cosmological constant from Figure 1 are listed in Table 2.

From Figure 1 and Table 2, we find that the current GRB sample place different constraints on  $\Omega_M$  and  $\Omega_\Lambda$  for different sets of  $(a, C)$ , indicating that  $a$  and  $C$  values are sensitive in constraining cosmology. Among the nine scenarios, the set of  $(1.5, 1.0)$  gives the lowest  $\chi^2_{\min}$ , which is 18.201 for 17 bursts. In this scenario, we measure  $\Omega_M = 0.18^{+0.18}_{-0.02}$  ( $1\sigma$ ) for a flat universe with a cosmological constant. This result is consistent with that from other observations. We also see that the set of  $(1.5, 0.8)$  gives the similar value of  $\chi^2_{\min}$ , which is 18.202 for 17 bursts. In this scenario, however, the flat universe model is ruled out at the  $1\sigma$  confidence level. The other cases also present meaningful results. Different GGL relations are sensitive enough to give different constraints on the cosmological parameters. This sensitivity implies that once the GGL relation is calibrated by a low-redshift sample, the GRB data will independently place its unique constraints on the universe, making GRBs a new cosmological ruler.

### 3.2.2. Exploring Dark Energy

When several non-interacting components are included in the universe, the Friedmann equations read

$$H^2(z) = H_0^2 \left[ \sum_{\alpha} \Omega_{\alpha} \exp \left\{ 3 \int_0^z \frac{dz'}{1+z'} [1+w_{\alpha}(z')] \right\} + \Omega_k (1+z)^2 \right] \quad (12)$$

$$\Omega_k = 1 - \sum_{\alpha} \Omega_{\alpha} \quad (13)$$

where  $\Omega_{\alpha}$  is the density parameter for the  $\alpha$ th component (e.g. matter, radiation, cosmological constant), and  $w_{\alpha}(z)$  is the corresponding equation of state (EOS) parameter. It is familiar that non-relativistic matter  $\Omega_M$  has  $w_M = 0$ , while a non-evolving cosmological constant  $\Omega_{\Lambda}$  has  $w_{\Lambda} = -1$ .

Current cosmological observations show a strong signature of the existence of a dark energy component with negative pressure. We assume a generalized dark-energy component which satisfies a constant equation of state,  $w = P/\rho c^2$ , with a flat universe. Therefore, we obtain the luminosity distance

$$d_L = c H_0^{-1} (1+z) \int_0^z dz [\Omega_M (1+z)^3 + (1-\Omega_M)(1+z)^{3(1+w)}]^{-1/2}. \quad (14)$$

It should be noted, from the above equation, that: (i) the acceleration of the universe requires  $w < -\frac{1}{3}$ , and (ii) all values of  $w$  other than  $w = -1$  lead to a dark energy density that evolves

as  $(1+z)^{3(1+w)}$ . The joint confidence intervals (after marginalizing over  $h$ ) in the  $\Omega_M - w$  plane for the nine sets of  $(a_i, C_i)$  are shown in Figure 2. Similar to Figure 1, we find that current GRB sample gives different constraints in the  $\Omega_M - w$  plane for different sets of  $(a, C)$ .

Figures 1 and 2 suggest that with different sets of  $(a, C)$  the GGL relation can be used to constrain  $\Omega_M$ ,  $\Omega_\Lambda$ , and even  $w$ . In the following, we consider a case of  $a \sim 1.5$  and  $C \sim 1.0$ , the lowest  $\chi^2_{\text{min}}$  case, as an example to present a further analysis. The Hubble diagram for this scenario (filled circles) is shown in Figure 3. For comparison, the binned SN Ia data taken from Riess et al. (2004) are also plotted (open circles). The solid curve in Figure 3 represents the theoretical Hubble diagram of the cosmic concordance model ( $\Omega_M = 0.27$ ,  $\Omega_\Lambda = 0.73$ , and  $h = 0.71$ ). As shown, the three Hubble diagrams are consistent with each other. This, together with the physical explanations (Dai et al. 2004; Rees & Mészáros 2004), implies that the present example seems to be favored. In this case, the value of  $w$  is less than  $-0.33$  (at  $\sim 1\sigma$ ). With a prior of  $\Omega_M = 0.27 \pm 0.04$  by assuming its Gaussian distribution (Riess et al. 2004), we obtain  $w = -0.98^{+0.44}_{-0.75}$  ( $1\sigma$ , see Figure 4). These results suggest that the cosmological constant appears to be a most competitive candidate of dark energy.

We consider the possibility that dark energy evolves with redshift. A simple and phenomenological procedure is to parameterize the function  $w(z)$  in some suitable form, and then determine the parameters in this function with the observational data. We first take the function as (Function I)

$$w(z) = w_0 + w'z \quad (15)$$

where  $w_0$  is the current EOS parameter, and  $w' \equiv \frac{dw}{dz}|_{z=0}$  gives its current evolution rate. In this case, the luminosity distance is given by

$$d_L = cH_0^{-1}(1+z) \int_0^z dz [\Omega_M(1+z)^3 + (1-\Omega_M)(1+z)^{3(1+w_0-w')} e^{3w'z}]^{-1/2} \quad (16)$$

Figure 5 shows the contours of likelihood intervals in the  $w_0 - w'$  plane for the case of  $a \sim 1.5$  and  $C \sim 1.0$  with a prior of  $\Omega_m = 0.27$  (solid contours, after marginalizing over  $h$ ). In this figure, the square marks the position of a cosmological constant  $(-1, 0)$ , which is within the contour of  $1\sigma$ . We see in this figure that  $w_0 > -1.50$  and  $w' < 1.43$  ( $1\sigma$ ).

We also take another form as (Function II)

$$w(z) = w_0 + w_1 \frac{z}{1+z} \quad (17)$$

to investigate the evolution of  $w$ , where  $w_0$  measures the current value of the parameter and  $w_1$  gives the current evolving rate. This parameterization indicates that  $w$  is finite in the

entire range of  $0 < z < \infty$ . The luminosity distance in this case is given by

$$d_L = cH_0^{-1} \int_0^z dz [\Omega_M(1+z)^3 + (1-\Omega_M)(1+z)^{3(1+w_0+w_1)} e^{-3w_1 z/(1+z)}]^{-1/2}. \quad (18)$$

The contours of the likelihood intervals in the  $w_0 - w_1$  plane with a prior of  $\Omega_M = 0.27$  for this case are also shown in Figure 5 (dashed contours, after marginalizing over  $h$ ), which yield  $w_0 > -1.72$  and  $w_1 < 3.58$  at the  $1\sigma$  confidence level. From Figure 5, we see that, joint constraints on both the recent equation of state of dark energy,  $w_0$ , and its time evolution,  $dw/dz$  or  $w_1$ , are consistent with the static nature, namely, value of  $w$  expected for a cosmological constant.

### 3.2.3. Determining the Transition Redshift

It is crucial to determine the transition redshift from the decelerating epoch into the accelerating phase in precise cosmology era. By using a form  $q(z) = q_0 + z (dq/dz)|_{z=0}$ , Riess et al. (2004) analyzed a gold sample of 157 SNe Ia, which is mainly composed of low-redshift sources, and found a transition redshift of  $z_t = 0.46 \pm 0.13$ . However, this form is suitable only for low-redshift sources. We also use a new expression,  $q(z) = q_0 + q_1 \frac{z}{1+z}$ , where  $q_0$  is the current deceleration factor and  $q_1$  gives its rate of change at the present epoch to study the transition redshift, which can be given by  $z_t = -q_0/(q_0 + q_1)$ . With this expression, we derive  $z_t = 0.45^{+0.05}_{-0.13}$  from the gold sample of SNe Ia, which is consistent with the result presented by Riess et al. (2004). The upper two panels in Figure 6 show the likelihood functions of  $z_t$  for the SN gold sample with the two expressions.

We use the two expansion forms to investigate the transition redshift from the current GRB data with the GGL relation in the scenario of  $(a, C) \sim (1.5, 1.0)$ . Using the former expansion, at the  $1\sigma$  confidence level, we get  $-1.02 < q_0 < 0.20$ ,  $-0.80 < dq/dz < 1.65$ . The likelihood function for the transition redshifts of  $[0.0, 5.0]$  gives  $z_t \sim 0.89$ . Considering the latter parameterization, at the  $1\sigma$  level, we measure  $-1.26 < q_0 < 0.52$  and  $-2.60 < q_1 < 3.70$ . In this case, the likelihood function for the transition redshifts of  $[0.0, 5.0]$  gives  $z_t \sim 0.66$ . The lower two panels in Figure 6 illustrate the likelihood function of  $z_t$  of  $[0.0, 1.0]$  (after applying 9 point Fast Fourier Transform smoothing).

As can be seen, even at the  $1\sigma$  confidence level, current GRB data cannot give a satisfactory constraint on the transition of the two epochs. However, our results reveal that the new parameterization trends to give more convincing constraints especially from high-redshift sources.

## 4. Simulations and Cosmological Applications

### 4.1. Procedure of Simulations

The different constraints from 17 observed GRBs with a fixed GGL relation motivate us to make a Monte Carlo simulation and thus use a large pseudo-GRB sample to present a further analysis. To compare the constraints from a GRB sample with those from SNe Ia, we generate a sample of 157 pseudo bursts.

Our simulations are based on the GGL relation in the cosmic concordance model from the GRB sample in Table 1. In this model, we find that  $a = 1.512$ ,  $C = 0.990$ ,  $\theta < 0.2$  rad, and  $E_{\gamma,\text{jet}} \in [6.38 \times 10^{49}, 8.47 \times 10^{51}]$  ergs. The observed peak energy  $E_p$  is of  $[35.0, 780.8]$  keV. These restrictive conditions are imposed upon our simulations. Each pseudo GRB is characterized by a set of  $S_b$ ,  $t_j$ ,  $n$ ,  $z$  and  $E_p$ , where  $S_b$  is the “bolometric” fluence in gamma-ray band. The procedure of our simulations is as follows:

(1) We derive the distributions of observational quantities  $S_b$ ,  $t_j$ ,  $n$ , and  $z$  and their uncertainties. It is impossible to establish robust distributions from the current GRB sample. From the 17 GRBs in Table 1, we find  $S_b \in [9.10 \times 10^{-7}, 6.08 \times 10^{-4}]$  erg cm $^{-2}$  with  $\langle \Delta S_b / S_b \rangle = 0.115 \pm 0.043$ , and  $t_j \in [0.43, 4.74]$  days with  $\langle \Delta t_j / t_j \rangle = 0.196 \pm 0.134$ . We thus simply assume that  $S_b$  and  $t_j$  uniformly distribute in these ranges with Gaussian distributions for their errors. Because  $n$  is unavailable in the literature for most GRBs, we take the distribution of  $n$  to be a random distribution in  $[1, 10]$  cm $^{-3}$  (e.g. Frail et al. 2001; Ghirlanda et al. 2004b) with a Gaussian distribution for  $\langle \Delta n / n \rangle = 0.5 \pm 0.2$ . The distribution of  $z$  is taken as the observational redshift distribution (Bloom et al. 2003) and the error of  $z$  is ignored in our simulations. We also get  $\langle \Delta E_p / E_p \rangle = 0.171 \pm 0.085$  from the 17 GRBs.

(2) We randomly generate a pseudo GRB characterized by a set of  $(S_b \pm \Delta S_b, t_j \pm \Delta t_j, n \pm \Delta n$  and  $z)$  from the distributions described in (1), compute its  $E_{\gamma,\text{jet}}$  with the cosmic concordance model, and then calculate its  $E_p$  by the GGL relation of  $(1.512, 0.990)$ .

(3) The pseudo GRB generated in step (2) strictly follows the GGL relation. We add a random deviation to each parameter to make this pseudo GRB more realistic, i.e.,  $S'_b = S_b + 0.8(-1)^m \Delta S_b$ ,  $t'_j = t_j + 0.8(-1)^m \Delta t_j$ , and  $n' = n + 0.8(-1)^m \Delta n$ , where  $m$  is randomly taken as 0 and 1. We then calculate  $\theta'$  and  $E'_{\gamma,\text{jet}}$ . We also add a random deviation to the  $E_p$  value obtained in step 2, i.e.,  $E'_p = E_p + 0.8(-1)^m \Delta E_p$ , where  $\Delta E_p / E_p$  is randomly selected according to its Gaussian distribution.

(4) Since  $\theta < 0.2$  rad,  $E_{\gamma,\text{jet}} \in [6.38 \times 10^{49}, 8.47 \times 10^{51}]$  erg and  $E_p \in [35.0, 780.8]$  keV for the 17 GRBs in Table 1, we require  $\theta'$ ,  $E'_{\text{jet}}$ , and  $E'_p$  of a pseudo GRB have to within

these ranges, respectively.

(5) Repeat steps (2)-(4) to generate a sample of 157 pseudo bursts.

We find the half-opening angles of the pseudo sample are also less than 0.22 rad for various cosmic models as in the observed sample. The  $E_{\gamma,\text{jet}}$  as a function of  $E_p(1+z)$  for the pseudo GRB sample is shown in Figure 7 (open circles). The 17 observed GRBs are also shown in Figure 7 (filled triangles). As can be seen, the two samples constitute a homogenous class.

The pseudo sample is cosmology-dependent because our simulations are based on the cosmic concordance model. The scatter of the GGL relation in the pseudo sample is less than that in the observed sample. The main reason is that, for the 17 GRB sample, the dispersion is mainly contributed by the four “outliers”; while for the pseudo sample, the bursts are distributed around the “rigid” GGL relation with a Gaussian distribution. Such a pseudo-GRB sample seems to be more realistic. The typical fractional uncertainties of  $a$  and  $C$  for the pseudo sample decrease to 0.02 and 0.05, which will be used in the following section 4.2.

#### 4.2. Test With Our Method

We examine the cosmological constraints derived from the pseudo sample with different scenarios of the GGL relation. Shown in Figure 8 are the 1 to  $3\sigma$  confidence contours (solid ellipses) in the  $(\Omega_M, \Omega_\Lambda)$  plane for the case of  $(a, C) \sim (1.5, 1.0)$ . The results are consistent with the cosmic concordance model of  $\Omega_M = 0.27$ ,  $\Omega_\Lambda = 0.73$  ( $\chi^2_{\text{dof}} = 176.48/155 \approx 1.14$ ), and provide evidence of current cosmic acceleration at the  $> 99.7\%$  confidence level. We measure  $\Omega_M = 0.27^{+0.02}_{-0.04}$  ( $1\sigma$ ) for a flat universe with a cosmological constant. Comparing to the results from the 17 GRBs (dashed contours), a larger sample with a similar observational accuracy can place very firm constraints on the universe. The results from the SN Ia gold sample are also shown in Figure 8 (the gray contours) for comparison. We see that both the pseudo-GRB sample and the SNe Ia gold sample can provide cosmological constraints at a comparable confidence level.

Shown in Figure 9 are the 1 to  $3\sigma$  confidence contours (solid ellipses) in the  $(\Omega_M, \Omega_\Lambda)$  plane for the case of  $(a, C) \sim (1.5, 0.8)$ . The symbols in Figure 9 are the same as that in Figure 8. We find the lowest  $\chi^2_{\text{dof}} = 176.83/155 \approx 1.14$  when  $\Omega_M = 0.39$  and  $\Omega_\Lambda = 0.54$ . For a flat universe with a cosmological constant, we measure  $\Omega_M = 0.39^{+0.12}_{-0.04}$  ( $1\sigma$ ). These results also confirm a great leap in constraining the cosmological parameters from a small sample to a large sample with a calibrated “standard candle” relation.

Moreover, we use the pseudo sample to determine the transition redshift by employing two expansion forms of  $q(z)$  (equations 15 and 17) in the case of  $a \sim 1.5$  and  $C \sim 1.0$ . The joint confidence contours in the  $dq/dz - q_0$  plane and the likelihood function of  $z_t$  are shown in Figure 10. We find  $z_t = 0.85^{+0.20}_{-0.17}$  when the expansion form of  $q(z)$  taken as equation (15), and  $z_t = 0.66 \pm 0.15$  when the expansion form of  $q(z)$  taken as equation (17). It seems that a high-redshift object would give a larger transition redshift compared with SN Ia.

### 4.3. Test with an Alternative Method

In Method I, the  $\chi^2$  statistic is written as:

$$\chi^2(\Omega_M, \Omega_\Lambda, a, C|h) = \sum_i \left[ \frac{\mu_{th}(z_i; \Omega_M, \Omega_\Lambda|h) - \mu_{obs}(z_i; \Omega_M, \Omega_\Lambda, a, C|h)}{\sigma_{\mu_{obs}}(\Omega_M, \Omega_\Lambda, a, C)} \right]^2, \quad (19)$$

where  $h$  is taken as 0.71. The procedure of this method is summarized as: (1) a best-fit of the GGL relation for a given cosmology of  $(\Omega_M, \Omega_\Lambda)_j$  is made to yield a set of  $(a, C)_j$  and  $(\sigma_a/a, \sigma_C/C)_j$ ; (2) the  $(a, C)_j$  and  $(\sigma_a/a, \sigma_C/C)_j$  are only used in the theoretical model of  $(\Omega_M, \Omega_\Lambda)_j$  to compute the bursts' apparent DMs and to further obtain the value of  $\chi_j^2$ ; and (3) the confidence contours are plotted according to the values of  $\chi_j^2$  in Step 2. Or without step 3, the confidence contours are plotted in step 2, according to the values of  $\chi^2$  which are given when performing the best-fits in step 1.

We apply this method for the 17 observed GRBs, and obtain the constraint on the mass density  $\Omega_M = 0.16^{+0.46}_{-0.14}$  ( $1\sigma$ ) for a flat universe. The lowest  $\chi_{dof}^2 = 17.33/15 \approx 1.16$  corresponds to a pair of  $\Omega_M = 0.16$  and  $\Omega_\Lambda = 0.42$ . This result is similar to that in Schaefer 2003 but with a higher observational accuracy. As shown in Figure 11 (dashed lines), the confidence contour intervals are much less stringent than those for fixed  $a$  and  $C$  (see Fig 1).

Furthermore, we consider this method for the pseudo sample, and the results are also shown in Figure 11 (solid confidence contours). The results are also consistent with the cosmic concordance model of  $\Omega_M = 0.27$  and  $\Omega_\Lambda = 0.73$  ( $\chi_{dof}^2 = 176.00/155 \approx 1.14$ ). We measure  $\Omega_M = 0.29^{+0.20}_{-0.04}$  ( $1\sigma$ ) for a flat universe with a cosmological constant. No convincing evidence for cosmic acceleration is provided at the  $2\sigma$  confidence level. Although more satisfactory results are obtained when using a large sample, Method I cannot give firm constraints comparable to Method II. This is easy to understand: in Method I, the  $\chi_j^2$  is always minimized for an assumed cosmic model of  $(\Omega_M, \Omega_\Lambda)_j$  by recalibration of the GGL relation and thus the values of  $\chi_{\min}^2$  derived from significantly different cosmic models are comparable.

The results with Method I are mainly affected by three factors: the redshifts of the

objects, the number of the objects and the observational accuracy. In the Hubble diagram, various cosmic models differ much as the redshift increases while degenerate more heavily as the redshift decreases. Thus, Method I will take effect for the high-redshift objects. However, we found that even when the redshifts of the pseudo bursts, selected according to the cosmic star formation rate, are up to  $z \sim 12$  (Prociani & Madau 2001), this method still cannot give evidence of cosmic acceleration at the 95.5% level. Therefore, although Method I opens a new methodology to measure cosmology, it seems that a calibration by a low-redshift sample cannot be leaped over for the GRB Cosmology, if any.

## 5. Conclusions and Discussion

We have shown that GRBs can measure cosmology using the tight GGL relation with either Method I or Method II. With Method II, we first analyzed this relation in various cosmic models to derive the distributions of  $a \in [1.40, 1.68]$  and  $C \in [0.70, 1.30]$ , and then considered nine representative sets of  $(a, C)$  and independently apply each set to the current GRB data for the cosmological test. We found that each case can give different constraints on the cosmological parameters, indicating the GGL relation appears to be tight enough to make GRBs a promising probe of the universe.

We have further considered the case of  $a \sim 1.5$  and  $C \sim 1.0$  as an example, and found that: (1) the mass density  $\Omega_M = 0.18 \pm 0.02^{0.18}$  ( $1\sigma$ ) for a flat universe with a cosmological constant; (2)  $w = -0.98^{+0.44}_{-0.75}$  ( $1\sigma$ ) with a prior of  $\Omega_M = 0.27 \pm 0.04$  for an assumed static equation of state of dark energy,  $P = w\rho c^2$ ; and (3) joint constraints on both the recent equation of state of dark energy,  $w_0$ , and its time evolution,  $dw/dz$  or  $-w_1$ , are consistent with the static nature, namely, value of  $w$  expected for a cosmological constant.

Furthermore, we carried out a simulation on the basis of the GGL relation in the cosmic concordance model. Our simulations show that although both methods, with a large sample, give more stringent constraints on the universe, the confidence intervals from Method I are much looser than that from Method II due to the method itself. Thus, if future observations on GRBs could calibrate  $a$  and  $C$  with a low-redshift sample (i.e.,  $z < 0.1$ ), Method II would be favored; if not, Method I would also provides unique cosmological constraints with a large sample.

The tight GGL relation implies that GRBs are a promising standard candle. The forthcoming *Swift* satellite is hopeful to catch more than 200 bursts during its nominal 2-year mission. It has the advantages of quick localization of bursts, continuous observation of X-ray and UV/optical afterglows at times of 1 minute to several days after the bursts, and

strong detectability of very high-redshift bursts. So, cornucopian observations for GRBs are expected to make a definite calibration in GRBs and a large observed sample into reality.

Finally, it should be pointed out that although the GGL relation seems to be tight enough for measuring cosmology, it strongly relies on the GRB afterglow jet model and various measurements. New relations, which should relate with as few well-observed quantities as possible, are required for improvement on this issue. In addition, the subject of possible cosmic evolution for one certain calibration is in need of a large observed sample with known redshifts.

XD is grateful to X.L. Luo for helpful discussions. This work was supported by the National Natural Science Foundation of China (grants 10233010, 10221001, and 10463001), the Ministry of Science and Technology of China (NKBRSP G19990754), the National Post Doctoral Foundation of China, and the Research Foundation of Guangxi University.

## REFERENCES

Amati, L. et al. 2000, *Science*, 290, 953  
Amati, L. et al. 2002, *A&A*, 390, 81  
Andersen, M. I. et al. 2003, *GCN*, 1993  
Atteia, J. L. 2003, *A&A*, 407, L1  
Barraud, C. et al. 2003, *A&A*, 400, 1021  
Barth, A. J. et al. 2003, *ApJ*, 584, L47  
Band, D.L., Matteson, J., Ford, L., et al. 1993, *ApJ*, 413, 281  
Bennett, C. L. et al. 2003, *ApJS*, 148, 1  
Berger, E. et al. 2001, *ApJ*, 556, 556  
Berger, E. et al. 2003, *Nature*, 426, 154  
Bjornsson G. et al. 2001, *ApJ*, 552, L121  
Bloom, J. S., Frail, D. A., & Sari, R. 2001, *AJ*, 121, 2879  
Bloom, J. S., Frail, D. A., & Kulkarni, S. R. 2003, *ApJ*, 594, 674

Branch, D., & Miller, D. L. 1993, ApJ, 405, L5

Bromm, V., & Loeb, A. 2002, ApJ, 575, 111

Carroll, S. M., Press, W. H., & Turner, E. L. 1992, ARA&A, 30, 499

Ciardi, B., & Loeb, A. 2000, ApJ, 540, 687

Crew, G. B. et al. 2003, ApJ, 599, 387

Dai, Z. G., & Lu, T. 2002, ApJ, 580, 1013

Dai, Z. G., Liang, E. W. & Xu, D. 2004, ApJ, 612, L101

Daly, R. A., Guerra, E. J., 2002, AJ, 124, 1831

Djorgovski, S. G. et al. 1998a, GCN, 189

Djorgovski, S. G. et al. 1998b, GCN, 137

Djorgovski, S. G. et al. 2001, ApJ, 526, 654

Eichler, D., & Levinson, A. 2004, preprint (astro-ph/0405014)

Filippenko, A. V. 1997a, in Thermonuclear Supernovae, ed. P. Ruiz-Lapuente et al. (Dordrecht: Kluwer), 1

Filippenko, A. V. 1997b, ARA&A, 35, 309

Filippenko, A. V. 2004, astro-ph/0410609

Frail, D. A., Waxman, E., and Kulkarni, S. R. 2000, ApJ, 537, 191

Frail, D. A. et al. 2001, ApJ, 562, L55

Frail, D. A. et al. 2003, ApJ, 590, 992

Freedman, W. L. 2001, ApJ, 553, 47

Friedman, A. S. & Bloom, J. S., astro-ph/0408413

Fruchter, A. et al. 1999, ApJ, 519, L13

Galama, T. J. et al. 1998, ApJ, 497, L13

Galama, T. J. et al. 1999, GCN, 338

Ghirlanda, G., Ghisellini, G., & Lazzati, D. 2004a, ApJ, in press

Ghirlanda, G. et al. 2004b, ApJ, 613, L13

Goldhaber, G., et al. 2001, ApJ, 558, 359

Greiner, J. et al. 2002, GCN, 1886

Greiner, J. et al. 2003, GCN, 2020

Halpern, J. P., et al. 2000, ApJ, 543, 697

Hjorth, J. et al. 1999, GCN, 219

Hjorth, J. et al. 2003, ApJ, 597, 699

Holland, et al. 2002, AJ, 124, 639

Holland, et al. 2003, AJ, 125, 2291

Holland, et al. 2004, astro-ph/0405062

Israel, G. L. et al. 1999, A&A, 348, L5

Jakobsson, S. P. et al. 2004, A&A, in press

Jimenez, R., Band, D. L., & Piran, T., 2001, ApJ, 561, 171

Klose, S. et al. 2004, astro-ph/0408041

Kirshner, R. P. 2003, Science 300, 1914

Kulkarni, S. R. et al. 1999, Nature, 398, 389

Lamb, D. Q., & Reichart, D. E. 2000, ApJ, 536, 1

Lamb, D. Q. et al. 2004, NewA Rev., 48, 423

Liang, E. W., Dai, Z. G., & Wu, X. F. 2004, ApJ, 606, L29

Lloyd-Ronning, N. M., Fryer, C. L. & Ramirez-Ruiz, E. 2002, ApJ, 574, 554

Macfadyen, A.I., Woosley, S.E. 1999, ApJ, 524, 262

Masetti, N. et al. 2000, A&A, 354, 473

Masetti, N. et al. 2002, GCN, 1330

Matheson, T. et al. 2003, ApJ, 582, L5

Panaitescu, A., & Kumar, P. 2002, ApJ, 571, 779

Perlmutter, S. et al. 1997, ApJ, 483, 565

Perlmutter, S. et al. 1999, ApJ, 517, 565

Phillips, M. M. 1993, ApJ, 413, L105

Porciani, C. & Madau, P. 2001, ApJ, 548, 522

Price, P. A. et al. 2002, ApJ, 573, 85

Price, P. A. et al. 2003, ApJ, 589, 838

Rees, M. J., & Mészáros, P. 2004, ApJ, submitted (astro-ph/0412702)

Rhoads, J. E. 1999, ApJ, 525, 737

Riess, A. G., Press, W. H., & Kirshner, R. P. 1996, ApJ, 473, 88

Riess, A. G. et al. 1998, AJ, 116, 1009

Riess, A. G. et al. 2004, ApJ, 607, 665

Rol, E. et al. 2003, GCN, 1981

Sakamoto, T. et al., 2004, ApJ, 602, 875

Sakamoto, T. et al., 2004a, astro-ph/0409128

Sari, R., Piran, T., & Halpern, J. P. 1999, ApJ, 519, L17

Sazonov, S. Y. et al. Nature 430, 646

Schaefer, B. E. 2003, ApJ, 588, 387

Schmidt, B. P. et al. 1998, ApJ, 507, 46

Soderberg, A. M. et al. Nature 430, 648

Spergel, D. N. et al. 2003, ApJS, 148, 175

Tegmark, M. et al. 2004, ApJ, 606, 702

Tiengo, A. et al. 2003, A&A, 409, 938

Tonry, J. T., et al. 2003, ApJ, 594, 1

Torii, T. et al. 2002, GCN, 1378

Vanderspek, R. et al. 2004, preprint (astro-ph/0401311)

van den Bergh, S., & Pazder, J. 1992, ApJ, 390, 34

Vreeswijk, P. M. et al. 1999a, GCN, 324

Vreeswijk, P. M. et al. 1999b, GCN, 496

Vreeswijk, P. M. et al. 2003, GCN, 1785

Waxman, E. et al. 1998, ApJ, 497, 288

Weidinger et al. 2003, GCN, 2215

Yamazaki, R., Ioka, K., & Nakamura, T. 2004, ApJ, 606, L33

Zhang, B. & Mészáros, P. 2002, ApJ, 581, 1236

Table 1. Sample of 17 GRBs

GRB	$z$	$E_p^{obs}(\sigma_{E_p^{obs}})$ [KeV] <sup>a</sup>	$[\alpha, \beta]$ <sup>a</sup>	$S_\gamma(\sigma_{S_\gamma})$ [ $10^{-6}$ erg cm $^{-2}$ ] <sup>b</sup>	bandpass [KeV] <sup>b</sup>	$t_j(\sigma_{t_j})$ days <sup>c</sup>	$n(\sigma_n)$ [cm $^{-3}$ ] <sup>d</sup>	References ( $z, E_p^{obs}, [\alpha, \beta], S_\gamma, t_{jet}, n$ ) <sup>e</sup>
grb970828	0.957	297.7(59.5)	-0.70, -2.07	96.0(9.6)	20-2000	2.2(0.4)	3.0(0.3)	01,18(23),23,27,01,No
grb980703	0.966	254.0(50.8)	-1.31, -2.40	22.6(2.26)	20-2000	3.4(0.5)	28.0(10.0)	02,18(23),23,27,28,28
grb990123	1.600	780.8(61.9)	-0.89, -2.45	300.0(40.0)	40-700	2.04(0.46)	3.0(0.3)	03,24,24,24,29,No
grb990510	1.6187	161.5(16.0)	-1.23, -2.70	19.0(2.0)	40-700	1.6(0.2)	0.29(0.14)	04,24,24,24,30,43
grb990705	0.843	188.8(15.2)	-1.05, -2.20	75.0(8.0)	40-700	1.0(0.2)	3.0(0.3)	05,24,24,24,31,No
grb990712	0.430	65.0(10.5)	-1.88,-2.48	6.5(0.3)	40-700	1.6(0.2)	3.0(0.3)	06,24,24,24,32,No
grb991216	1.020	317.3(63.4)	-1.23, -2.18	194.0(19.4)	20-2000	1.2(0.4)	4.7(2.8)	07,18(23),23,27,33,43
grb011211	2.140	59.2(7.6)	-0.84, -2.30	5.0(0.5)	40-700	1.50(0.02)	3.0(0.3)	08,18,18,27,34,No
grb020124	3.200	120.0(22.6)	-1.10, -2.30	6.8(0.68)	30-400	3.0(0.4)	3.0(1.0)	09,(18)25,25,25,35,No
grb020405	0.690	192.5(53.8)	0.00, -1.87	74.0(0.7)	15-2000	1.67(0.52)	3.0(0.3)	10,19,19,19,19,No
grb020813	1.250	212.0(42.0)	-1.05, -2.30	102.0(10.2)	30-400	0.43(0.06)	3.0(0.3)	11,(18)25,25,25,36,No
grb021004	2.332	79.8(30.0)	-1.01, -2.30	2.55(0.60)	2 -400	4.74(0.14)	30.0(27.0)	12,20,20,20,37,44
grb021211	1.006	46.8(5.5)	-0.805,-2.37	2.17(0.15)	30-400	1.4(0.5)	3.0(0.3)	13,26,26,26,38,No
grb030226	1.986	97.1(20.0)	-0.89, -2.30	5.61(0.65)	2 -400	1.04(0.12)	3.0(0.3)	14,20,20,20,39,No
grb030328	1.520	126.3(13.5)	-1.14, -2.09	37.0(1.40)	2 -400	0.8(0.1)	3.0(0.3)	15,20,20,20,40,No
grb030329	0.1685	67.9(2.2)	-1.26, -2.28	110.0(10.0)	30-400	0.5(0.1)	1.0(0.11)	16,22,22,22,41,45
xrf030429	2.6564	35.0(9.0)	-1.12, -2.30	0.85(0.14)	2 -400	1.77(1.0)	3.0(0.3)	17,20,20,20,42,No

| 21 |

<sup>a</sup>The spectral parameters fitted by the Band function. The spectra of GRB020124, GRB020813, GRB021004, GRB030226, and XRF030429 are calculated by the Band function with  $\beta \sim -2.3$ . For GRB011211,  $\beta$  is taken to be -2.3 for no available in the literature.  $E_p^{obs}$  errors are assumed to be 20% when not reported in the literature. The error of  $k$ -correction is fixed at 5%.

<sup>b</sup>The fluences and their errors in the observed energy band. The errors are taken as 10% when no available in the literature. The Fluences and the spectral parameters are given from the same original literature as possible. For GRB

970828, GRB 980703, GRB 991216, and GRB 011211, their the fluences and spectral parameters are not presented in the same original paper, literature, we then choose their fluences observed in the widest energy band.

<sup>c</sup>Afterglow break times and errors in the optical band.

<sup>d</sup>The circum-burst medium density and error from broadband modelling of the afterglow light curves. If no available the value of  $n$  is taken as  $3 \pm 0.3 \text{ cm}^{-3}$ .

<sup>e</sup>References in order for  $z$ ,  $E_p^{obs}$ ,  $[\alpha, \beta]$ ,  $S_\gamma$ ,  $t_j$ , and  $n$ .

References. — (1) Djorgovski et al. 2001; (2) Djorgovski et al. 1998; (3) Hjorth 1999; (4) Vreeswijk et al. 1999a; (5) Amati et al. 2000; (6) Galama et al. 1999; (7) Vreeswijk et al. 1999b; (8) Holland et al. 2002; (9) Hjorth et al. 2003; (10) Masetti et al. 2002; (11) Price et al. 2002; (12) Matheson et al. 2003; (13) Vreeswijk et al. 2003; (14) Greiner et al. 2002; (15) Rol et al. 2003; (16) Greiner et al. 2003; (17) Weidinger et al. 2003; (18) Amati 2004; (19) Price et al. 2003; (20) Sakamoto et al. 2004a; (21) Atteia 2003; (22) Vanderspek et al. 2004; (23) Jimenez et al. 2001; (24) Amati et al. 2002; (25) Barraud et al. 2003; (26) Crew et al. 2003; (27) Bloom et al. 2003; (28) Frail et al. 2003; (29) Kulkarni et al. 1999; (30) Israel et al. 1999; (31) Masetti et al. 2000; (32) Bjornsson et al. 2001; (33) Halpern et al. 2000; (34) Jakobsson et al. 2003; (35) Torii et al. 2002; (36) Barth et al. 2003; (37) Holland et al. 2003; (38) Holland et al. 2004; (39) Klose et al. 2004; (40) Andersen et al. 2003; (41) Berger et al. 2003; (42) Jakobsson et al. 2004; (43) Panaitescu & Kumar 2002; (44) Schaefer et al. 2003; (45) Tiengo et al. 2003

Table 2: Comparison of constraints by using different calibrations

	$a$	$C$	$\Omega_M$	$\Omega_\Lambda$	$\chi^2_{min}$	$\Omega_M$ ( $1\sigma$ , flat universe)
<b>A</b>	1.4	1.2	0.20	0.72	20.25	$0.20^{+0.01}_{-0.13}$
<b>B</b>	1.4	1.0	0.23	0.11	19.39	$0.23^{+0.13}_{-0.07}$
<b>C</b>	1.4	0.8	0.28	-1.00	19.13	Rejected
<b>D</b>	1.5	1.2	0.15	0.92	18.61	$0.15^{+0.07}_{-0.08}$
<b>E</b>	1.5	1.0	0.18	0.45	18.201	$0.18^{+0.18}_{-0.02}$
<b>F</b>	1.5	0.8	0.15	-0.66	18.202	Rejected
<b>G</b>	1.6	1.2	0.11	1.08	18.36	$0.11^{+0.02}_{-0.08}$
<b>H</b>	1.6	1.0	0.14	0.73	18.32	$0.14^{+0.12}_{-0.05}$
<b>I</b>	1.6	0.8	0.11	-0.19	18.69	[0.28, 0.41]

<sup>1</sup>A latest sample of 17 GRBs analyzed.

<sup>2</sup>The best-fit set of  $[\Omega_M, \Omega_\Lambda]$  in the case of (1.4, 0.8) is below the line of  $\Omega_\Lambda = -1$ , because  $\Omega_\Lambda$  runs from -1 to 1.8 when we plot the contours in the  $\Omega_M - \Omega_\Lambda$  plane.

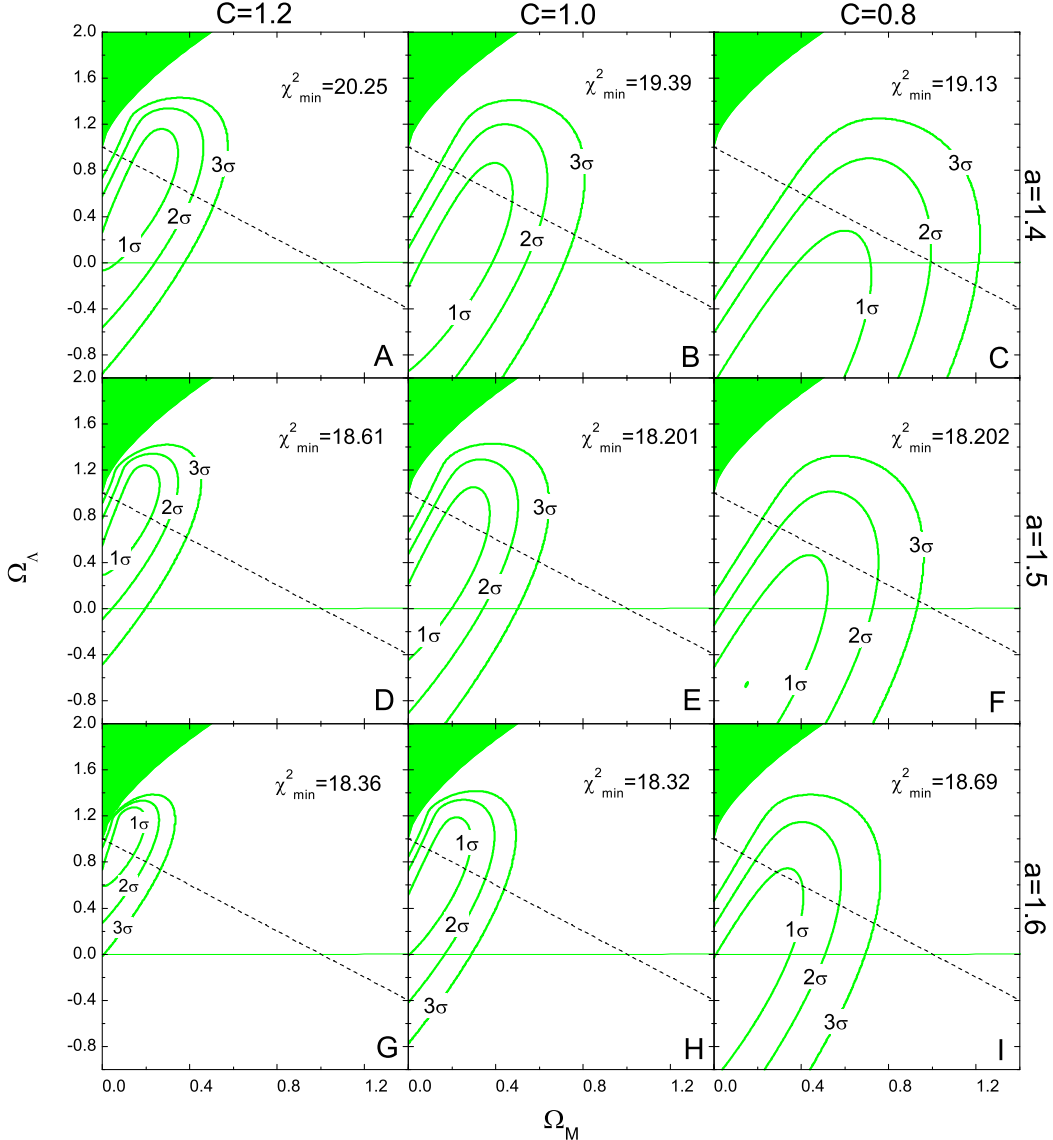


Fig. 1.— Joint confidence intervals from 1 to  $3\sigma$  for  $(\Omega_M, \Omega_\Lambda)$  from the observed GRB sample (17 bursts) with nine representative cases of the potential “standard candle” relation. Regions representing specific cosmological scenarios are also illustrated. Contours are closed by their intersection with the lines  $\Omega_M = 0$  and  $\Omega_\Lambda = -1$ .

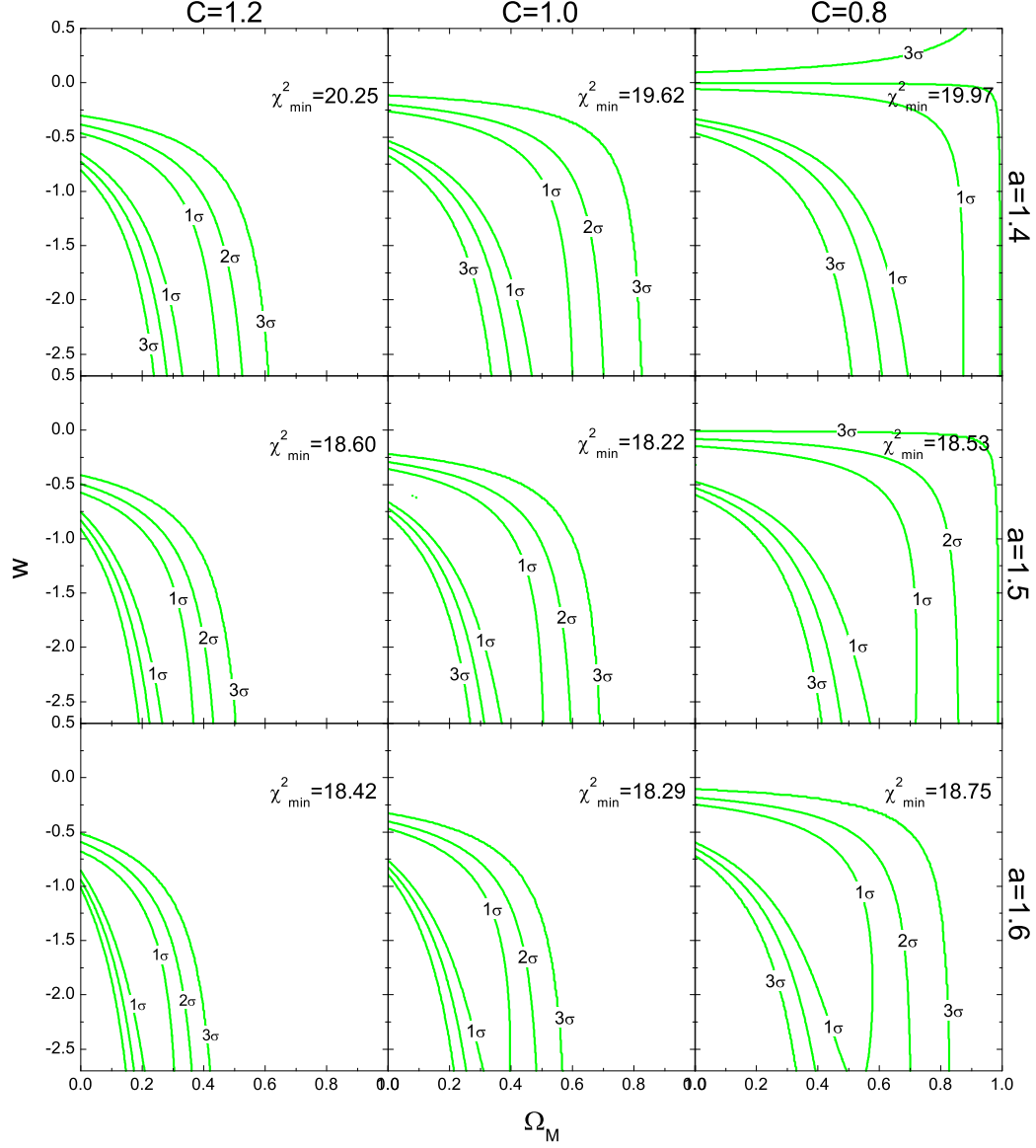


Fig. 2.— Joint confidence intervals from 1 to  $3\sigma$  for  $(\Omega_M, w)$  from the observed GRB sample (17 bursts) with the same nine potential calibrations as in Fig 1. In each case, a minimum  $\chi^2$  and the parameterization of the relation are marked.

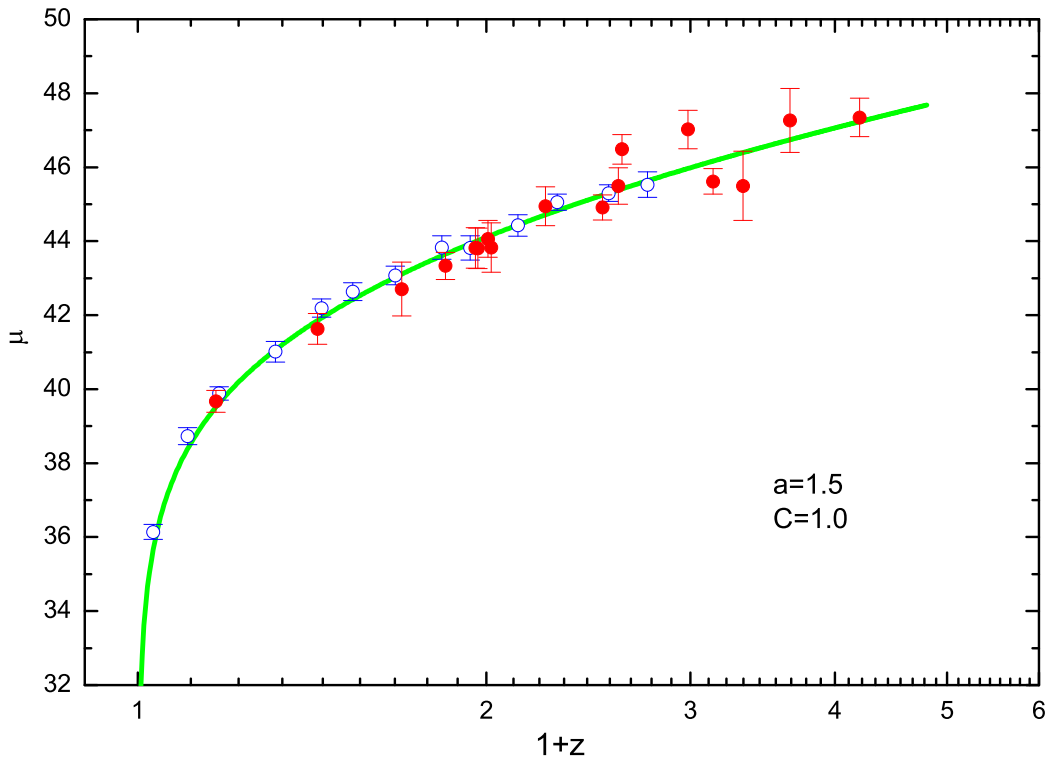


Fig. 3.— Hubble diagrams for the observed GRB sample (filled circles) with the (1.5, 1.0)-parametrizing calibration, and for the binned SN Ia GOLD sample from Riess et al. 2004 (open circles). The line represents a cosmic concordance model of  $\Omega_M = 0.27$ ,  $\Omega_\Lambda = 0.73$ , and  $h = 0.71$ .

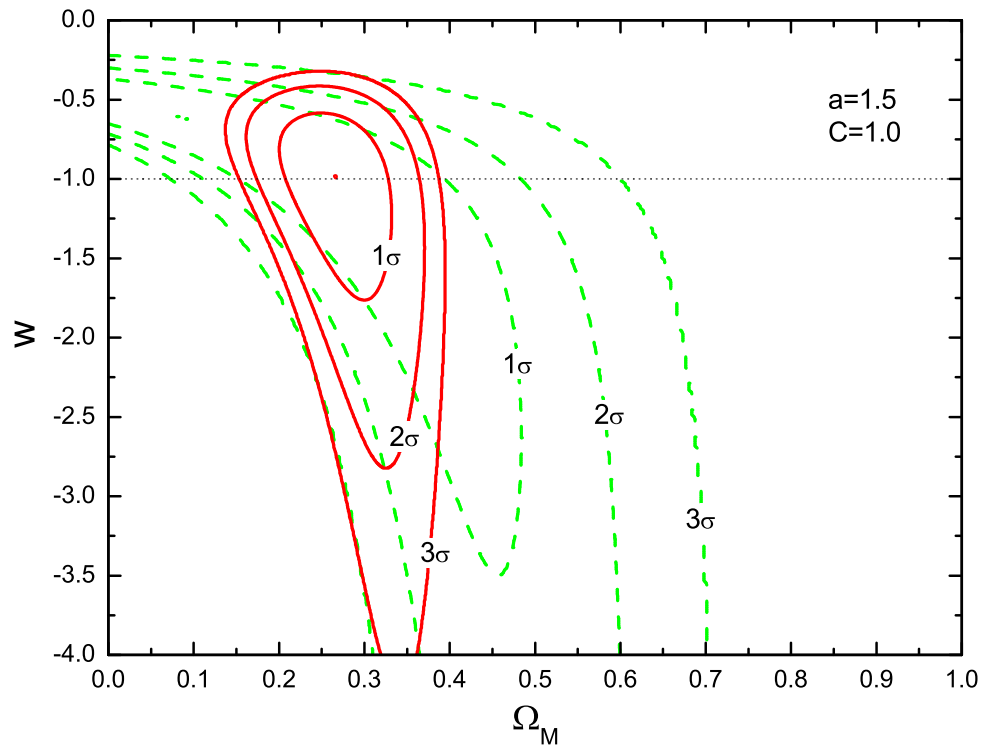


Fig. 4.— Confidence contours of likelihood from the observed GRB sample (dashed lines) in the  $\Omega_M$ - $w$  plane using the (1.5, 1.0)-parametrizing calibration. The solid contours are derived by considering a prior of  $\Omega_m = 0.27 \pm 0.04$ .

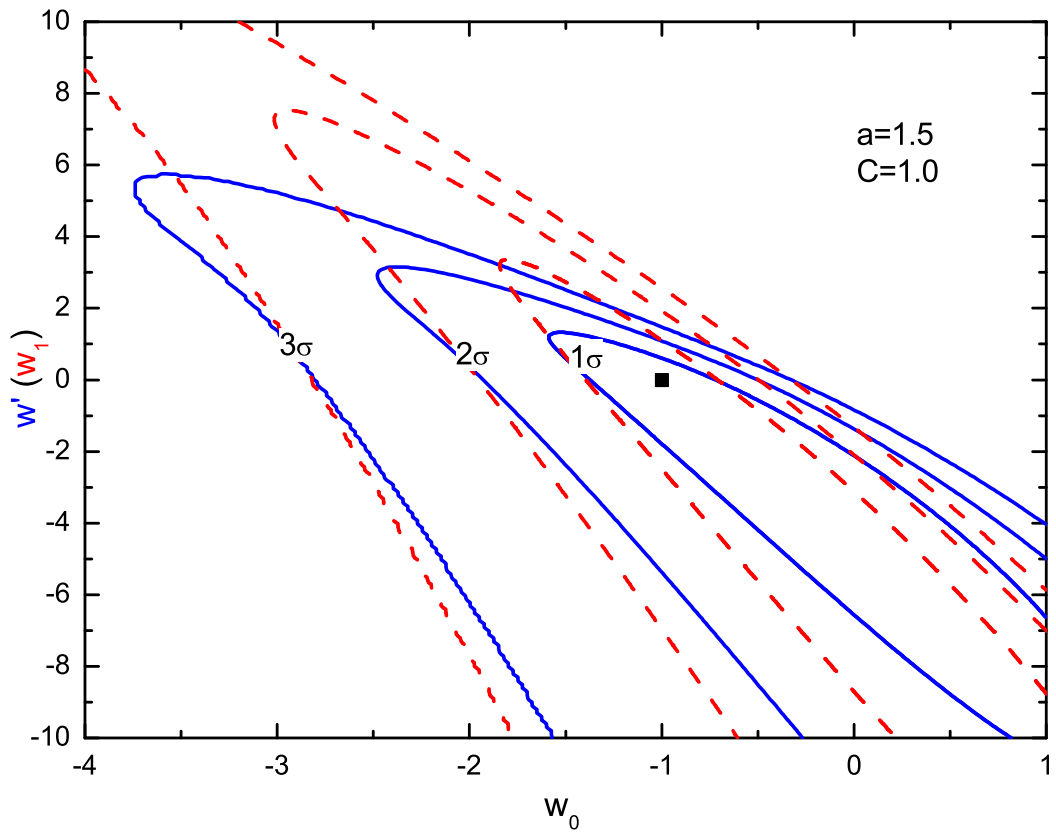


Fig. 5.— Joint confidence intervals for  $(w_0, w')$  and  $(w_0, w_1)$  from the observed GRB sample by using the same potential calibration in Fig 4. The solid contours of likelihood are calculate by using the expansion form of Function I together with a prior of  $\Omega_m = 0.27$ , and the dashed contours are derived by using Function II with the same prior.

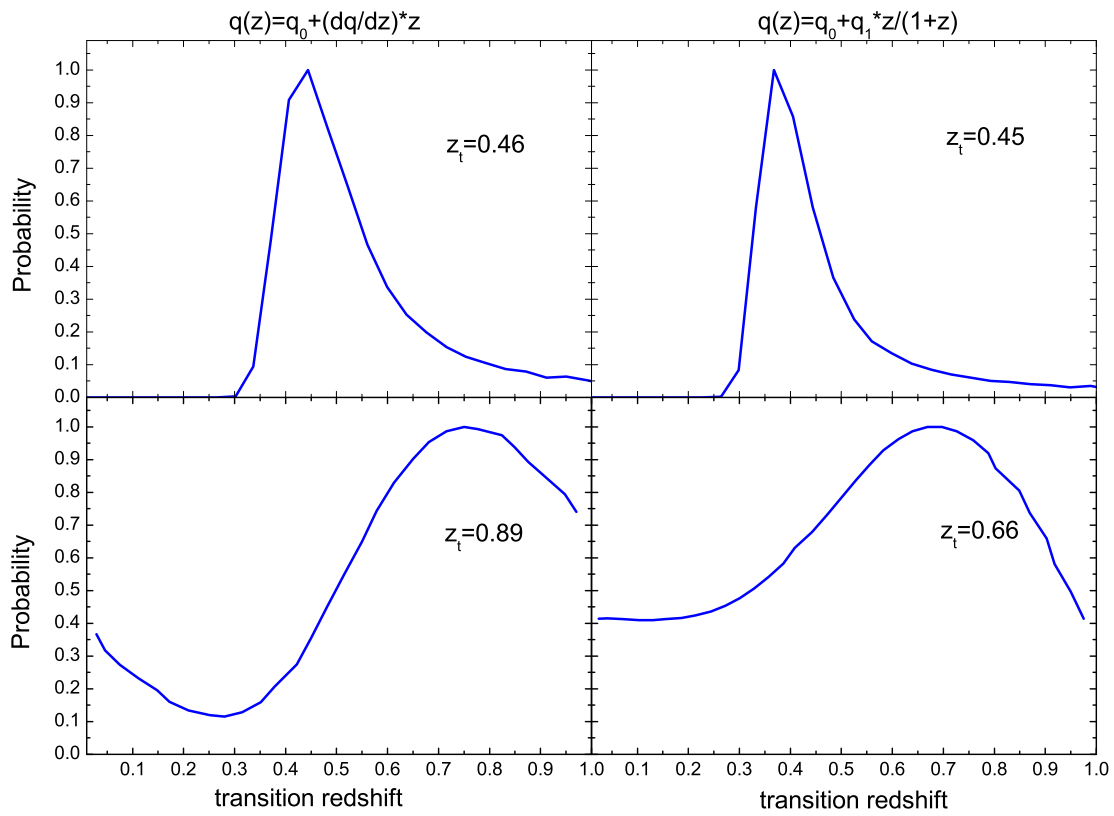


Fig. 6.— The likelihood functions of the transition redshifts for the SN Ia GOLD sample (upper panels) and for the observed GRB sample (lower panels): the left panels are computed by the same method as Riess et al. 2004, and the right panels are calculated by a new parametrization suggested in this paper.

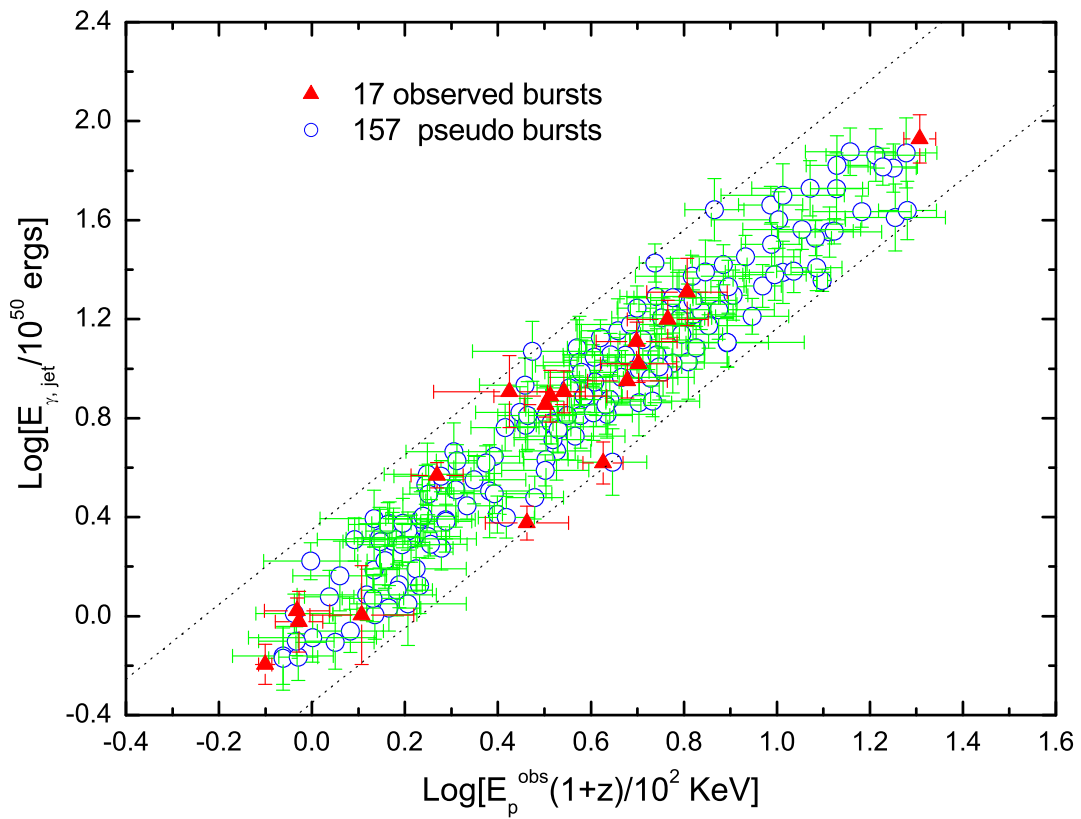


Fig. 7.—  $E_{\gamma, \text{jet}}$  as a function of  $E'_p$  measured in the rest frame for the pseudo GRB sample. The observed GRB sample is also plotted (the solid triangles) for comparison.

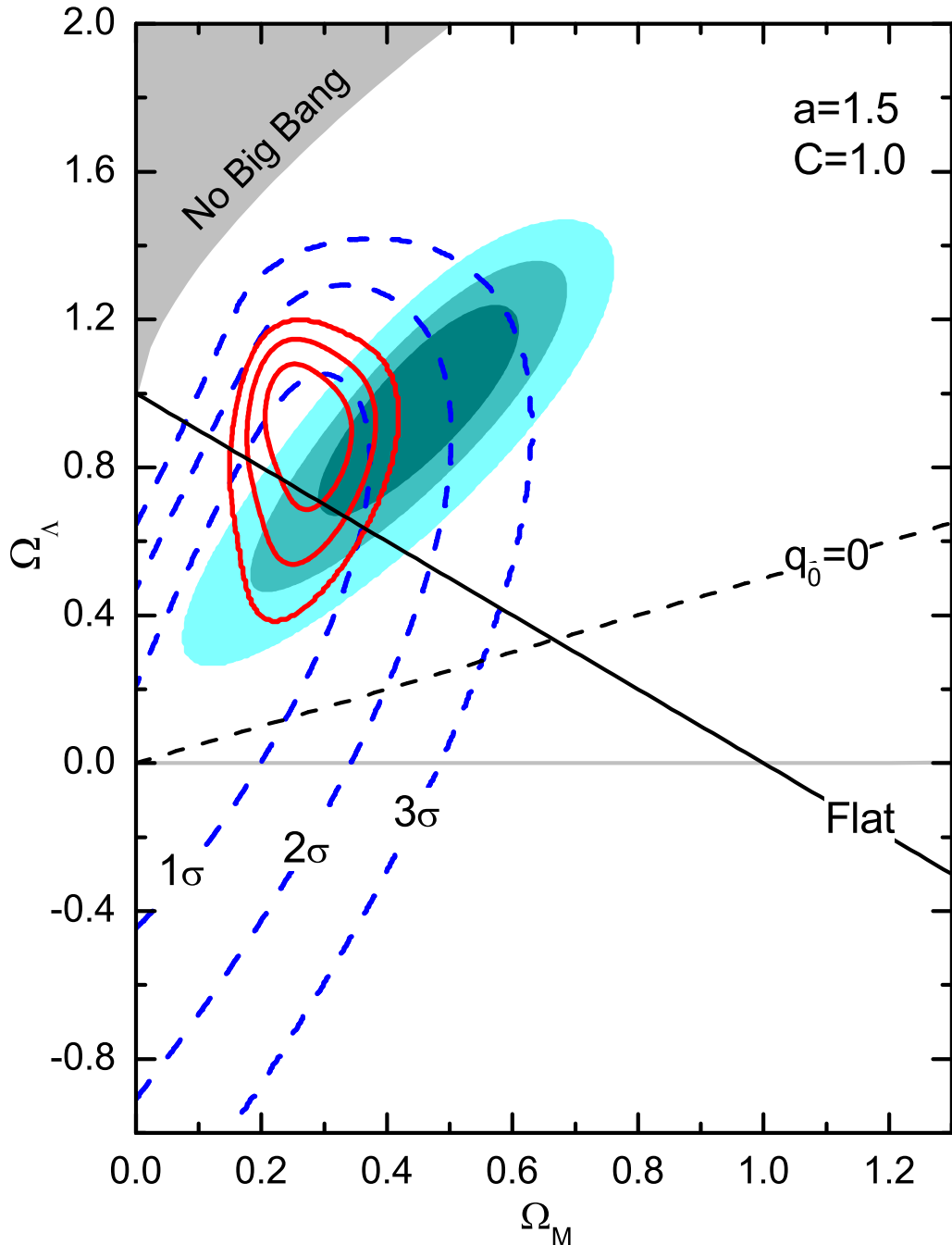


Fig. 8.— Joint confidence intervals for  $(\Omega_M, \Omega_\Lambda)$  from the pseudo GRB sample (solid contours, 1 to  $3\sigma$ ) and from the observed GRB sample (dotted contours), both considering the potential calibration of  $(1.5, 1.0)$ . The results from the SN Ia GOLD sample is also plotted for comparison (shaded contours).

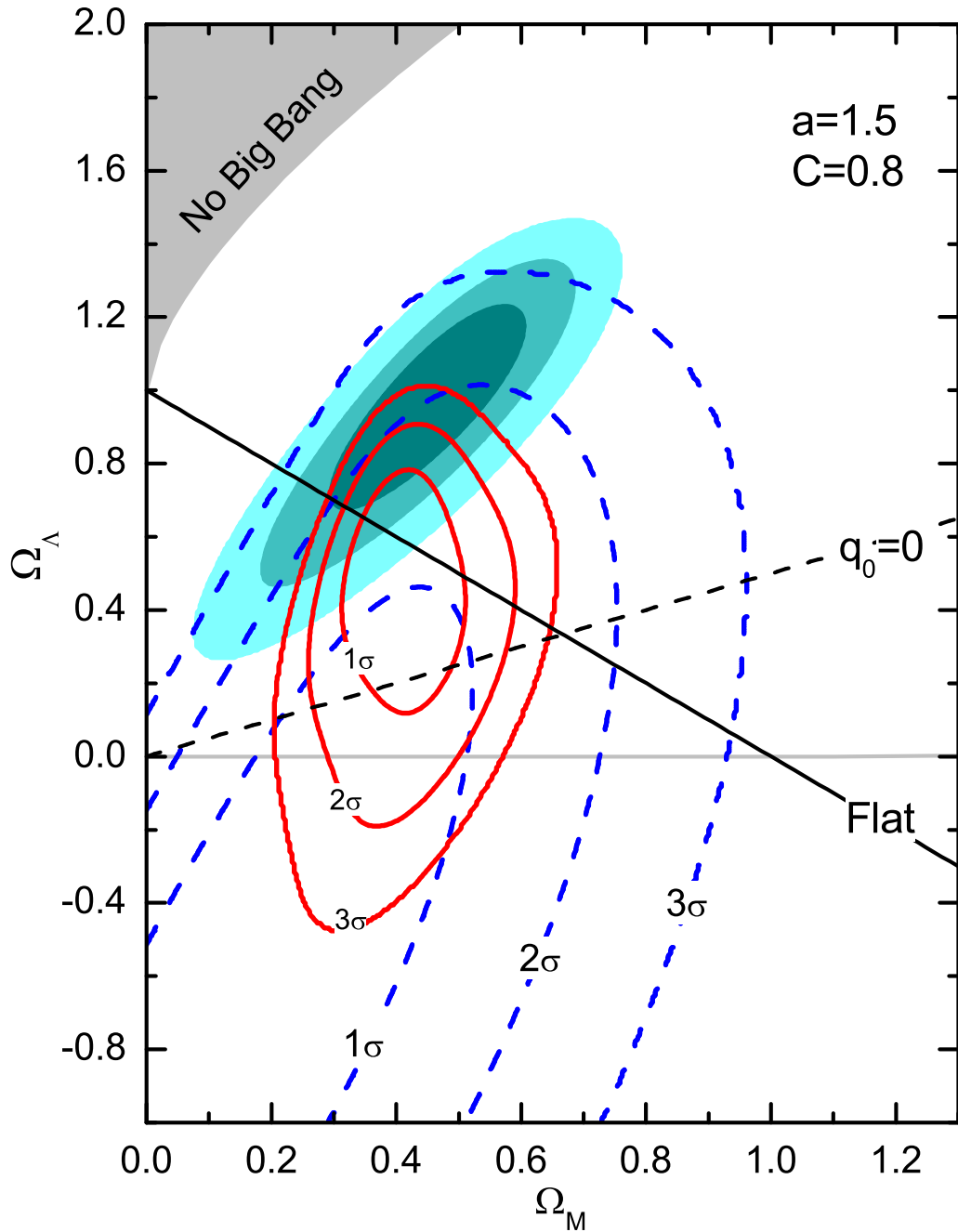


Fig. 9.— Joint confidence intervals for  $(\Omega_M, \Omega_\Lambda)$  from the pseudo GRB sample (solid contours) and from the observed GRB data (dotted contours), both employing the potential calibration of  $(1.5, 0.8)$ . Shaded confidence regions (1 to  $3\sigma$ ) are from the SN Ia GOLD sample.

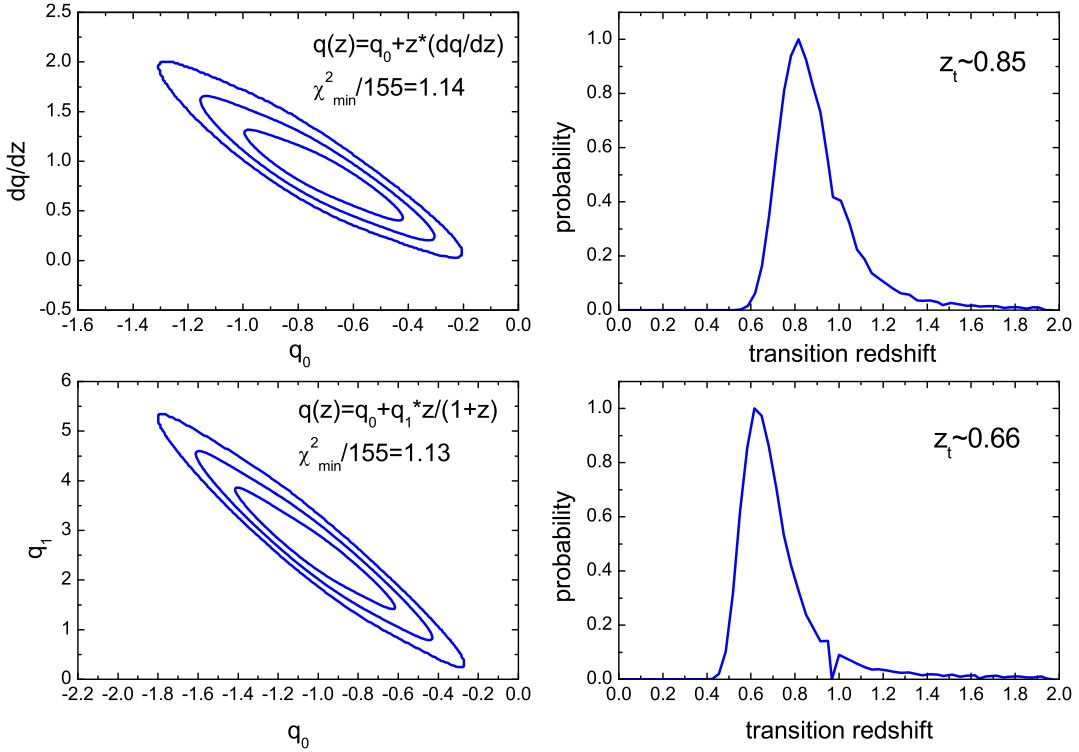


Fig. 10.— Upper two panels: Shown in the left are joint confidence intervals (1 to 3 $\sigma$ ) for  $(q_0, dq/dz)$  from the pseudo GRB sample using a calibration of (1.5, 1.0), and the right panel is the corresponding likelihood function of the transition redshift. Shown in the lower two panels are similar to the upper two but with the new parametrization of  $(q_0, q_1)$ .

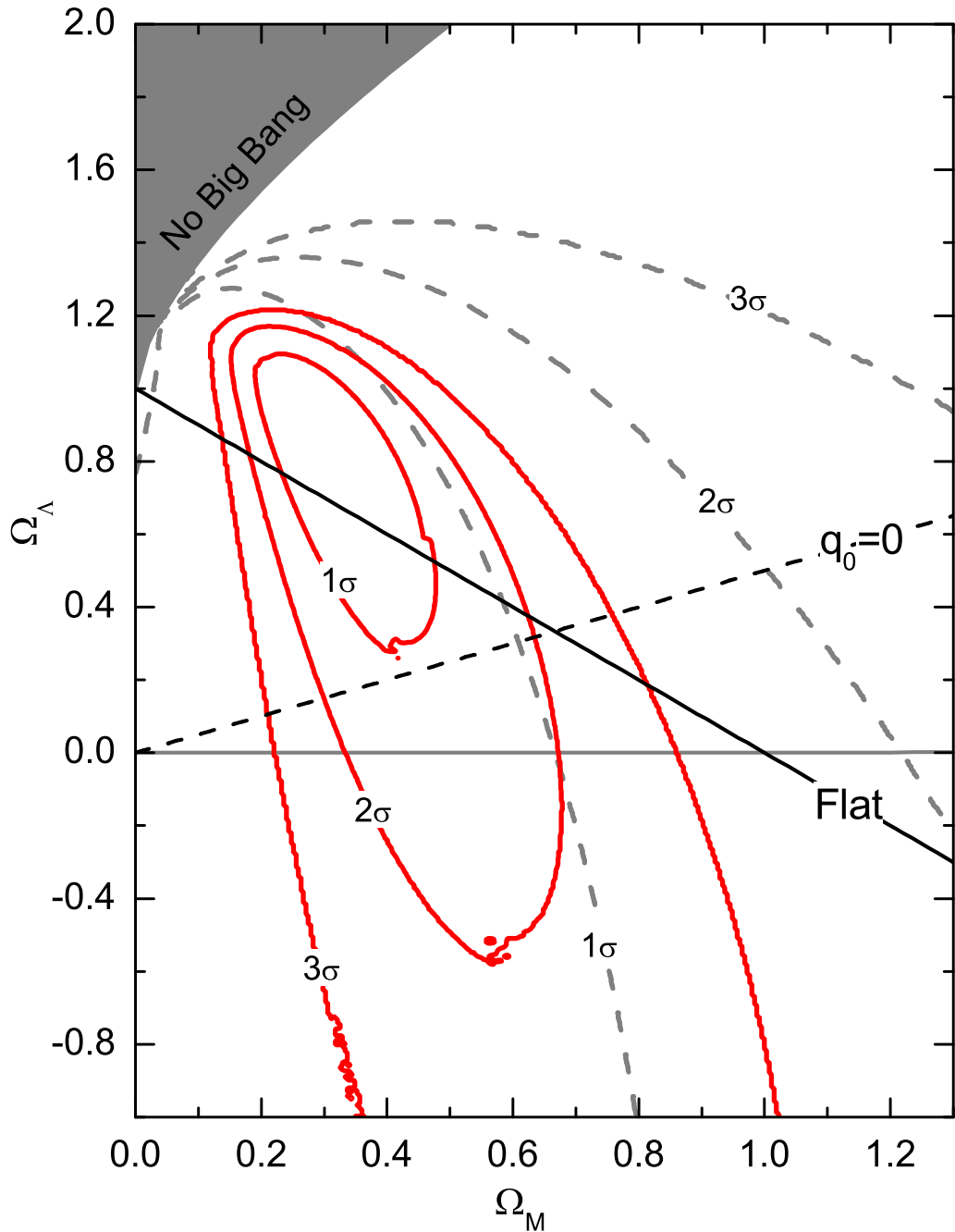


Fig. 11.— Joint confidence intervals for  $(\Omega_M, \Omega_\Lambda)$  from the pseudo GRB sample (solid contours) and from the observed GRB sample (dashed contours), both without the assumption of a calibrated “standard candle” relation.